ナノダイヤモンド膜の光電変換素子および硬質被膜への応用

吉武 剛
九州大学 大学院総合理工学研究院 エネルギー科学部門

ダイヤモンドは宝石として古より重宝されてきたが、昨今はその極めて優れた物性が注目を集め様々な分野への応用が期待されている。具体的には、i) 5.47 eV の大きなバンドギャップと高い絶縁破壊電圧を有することから究極の性能を有するパワーエレクトロニクス用のワイドギャップ半導体として、ii) 最高の熱伝導性を有することからヒートシンク材として、iii) 最高の硬さと耐摩耗性を有することから硬質被膜材料として、iv) 極めて高い化学安定性を有することから人工関節等への生体材料として、注目を集めている。特筆すべきは、上記のどの応用に関しても、ダイヤモンドは最高のポテンシャルを有するために、その応用に関する究極の材料といえる点である。

ダイヤモンドの中でも直径 10 nm 以下のダイヤモンド(ultrananocrystalline diamond: UNCD)と水素化アモルファスカーボン(a-C:H)マトリックスから成る超ナノ微結晶ナノダイヤモンド/水素化アモルファスカーボン混相(UNCD/a-C:H)膜は、ダイヤモンドおよびアモルファスカーボン単体と異なる性質を有する。UNCD/a-C:H 膜の特徴としては、(a) 一般的なアモルファスカーボン膜と同様に基板選択性が低いこと、(b) 多結晶ダイヤモンド膜とは対照的に平滑な表面を有すること、(c) 膜中に多数存在する UNCD 結晶の界面および粒界が原因と考えられる高い光吸収係数を有すること、(d) ターゲット材料であるグラファイトに異種元素を混ぜ込むことによって容易にドーピングが可能であること、が挙げられる。UNCD/a-C:H 膜の成膜は、単結晶および多結晶ダイヤモンド膜の研究の延長として、ほとんどが化学気相成長(CVD)法により行われてきた。それに対して、我々はこれまでの研究で、物理気相成長(PVD)法であるレーザーアブレーション法(pulsed laser deposition: PVD)法と同軸型アークプラズマ堆積(coaxial arc plasma deposition: CAPD)法を用いて UNCD/a-C:H 膜の成長を実現している。

PVD 法で作製される UNCD/a-C:H 膜は、ダイヤモンドの粒径が小さく、膜中に内在する無数のダイヤモンド微結晶の界面・粒界の効果が顕著である。それが原因で発現すると考えられる上記の c)、d)の特徴から、光電変換素子材料として面白いと考えている。炭素は放射線に対して極めて強い耐性があり、核廃棄物からの放射線を利用したダイヤモンド電池が現在注目を集めているが、大面積化が容易であることからそれへの応用に期待出来る。UNCD/a-C:H 膜に関する伝導型制御からフォトダイオード作製までの結果を報告する。

CAPD 法では非加熱基板上に、基板の温度がほとんど上昇することなくナノダイヤモンド膜を成長出来る。その利点を生かして、超硬合金へのハードコーティングとしての応用を検討している。近年の研究により、70 GPa の硬度の膜を 10 μm 以上の膜厚で堆積する技術を確立し、実用化に近いレベルまできた。最近の研究成果に関して紹介する。

ナノダイヤモンド膜の光電変換素子および硬質被膜への応用

吉武 剛

九州大学大学院 総合理工学研究院 エネルギー科学部門
［教育］大学院総合理工学府 量子プロセス理工学専攻
（総合理工学専攻 from 2021）
工学部 電気情報工学科
（融合基礎工学科 from 2021）
［研究］シンクロトロン光利用研究センター
日本エジプト科学技術連携センター
エネルギー基盤技術国際教育研究センター
〒816-8580 福岡県春日市春日公園６－１
総合研究棟（C-Cube）五階506室
☎ 092-583-8845
✉ tsuyoshi_yoshitake@kyudai.jp

Content

Researches on nanodiamond

- PVD Growth & Process diagnostics
- Hard coating
- Coating for biomedical
- Photovoltaics

Summary

Diamond excellent properties

Electr.	Wide-gap semiconductor with Eg = 5.47 eV Breakdown field 10 MV/cm Large electron mobility 2,200 cm^2/Vs Negative electron affinity High radiation-resistance	Power SC SC operating at high temp Radiation-resist SC PV for nuclear wastes
Mech.	Highest hardness 100 GPa Low friction coefficients Large elastic modulus Largest Sonic speed	Hard coating Biomedical coating SAW devices
Therm.	Highest thermal cond 20 W/cm K lowest thermal exp coefficient 8×10^{-7} K^{-1}	Heat sink
Chem.	Extremely stable Extremely large potential window	Electrode 4 electrolysis Biomedical mat
the others	Quantum centers w/ η = 100%	New mag field sensing Luminescent markers Quantum computing

---

Various nanocarbons

Nanocrystalline diamond (NCD)
< 100 nm

Ultrananocrystalline diamond (UNCD)
< 10 nm

Diamondoid
< 2 nm

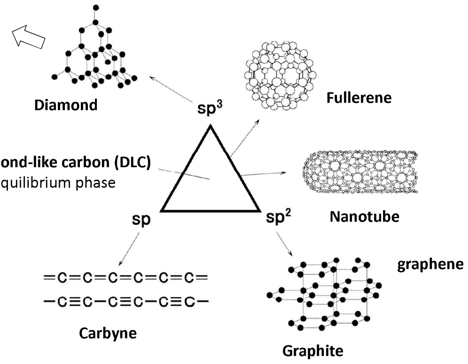

High temp. & high pressure
Stable phase

Diamond-like carbon (DLC)
Nonequilibrium phase

TEM images of UNCD/a-C:H films prepared by PLD

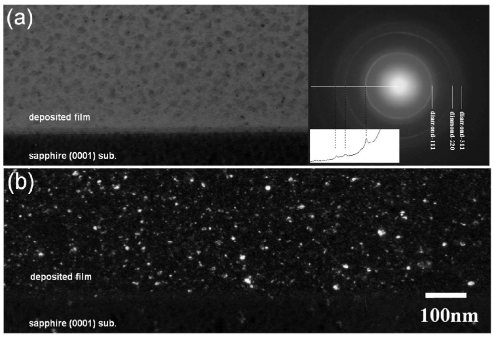

a) BF image and ED pattern, and (b)DF image using a portion of d-111 diffraction ring.

The existence of a huge number of GBs is structural specific to UNCD/a-C:H films. Here, GBs specifically denote the interfaces between UNCD grains and those between UNCD grains and an a-C:H matrix.

Comparison among DLC, UNCD/a-C:H, and diamond

UNCD/a-C:H films comprise diamond grains with diameters of less than 10 nm and an a-C:H matrix.

	DLC (a-C:H)	UNCD/a-C:H	Polycrystalline diamond	Singlecrystalline diamond
Structure	Amorphous	Nanocrystalline/ amorphous composite	Polycrystalline	Singlecrystalline
Growth on foreign substrates	Easy	Seeding required(CVD) Easy (PVD)	Seeding indispensable	Extremely difficult
Thermal stability	200-300 °C	550 °C ? (growth temp.)	800 °C	800 °C
Bandgap	Variable 0〜4 eV	1-3 eV	5.5 eV	5.5 eV
Absorption coefficient	Small	Large	Small	Small
control of conduction type	Insulating difficult	Both: possible?	n-Type: difficult	n-Type: difficult
Surface smoothness	Extremely smooth	Smooth	Rough	Extremely smooth

Progress of nanodiamond research

Film growth & Process

- Growth of UNCD/a-C:H films by PLD and CAPD
- Diagnostics of plasma deposition processes

T. Yoshitake et al., JJAP46 (2007) L936
K. Hanada et al., JJAP49 (2010) 08JF09
T. Yoshitake et al., JJAP49 (2010) 015503 etc.

Structures & Elem. prop.

- TEM observation
- Spectroscopic evaluations
- Measurement of elemental physical properties

T. Yoshitake et al., JJAP48 (2009) 020222
S. Ohmagari et al., J. Nanomater 2009 (2009) 876561
S. Al-Riyami et al., Diamond Rel. Mat. (2010) 510
Ali M. Ali et al, APL 116 (2020) 041601

Semicond.

- Control in the conduction type by N and B doping
- Study of the origin of the p- and n-type conduction

S. Al-Riyami et al, APEX 3 (2010) 115102
H. Gima et al, APEX 10 (2017) 015801

Device Fab.

- Fabrication of **heterojunction PD** with Si
- **Photodetection evaluation as UV sensors**

S. Ohmagari et al., APEX 6 (2012) 065202
Abdelrahman et al, APEX 8 (2015) 095101
Abdelrahman et al, Appl. Phys. A 123 (2017) 167

PV for nuclear wastes

Sensing under rad. cond.

- JST ALCA, 2011～13
- JSPS Grant-in-Aid for Sci. Res. (B), 2015～17
- JSPS Grant-in-Aid for Sci. Res. (B), 2019～22

Mech.

- Room-temp. deposition of 50 GPa hardness films on WC-Co sub.
- 60 GPa hardness & 10 μm thickness deposition owing to Si and B doping
- More than 70 GPa hardness by employing negative-bias applications.

H. Naragino et al., JJAP 55 (2016) 030302
M. Egiza et al. JJAP 58 (2019) 075507
Ali M. Ali et al, APEX13 (2020) 065506.

Hard coating for mechanical cutting tools

Biomedical coating for implants & artificial joints

・JST Value Progrum, 2016
・JST A-STEP ステージⅡ, 2017～22

Pulsed laser deposition (PLD)

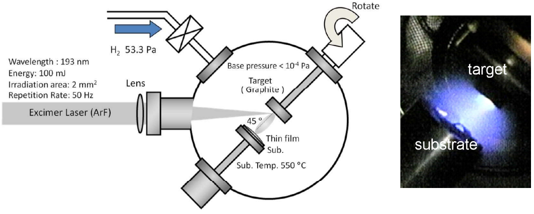

Coaxial Arc Plasma Deposition (CAPD)

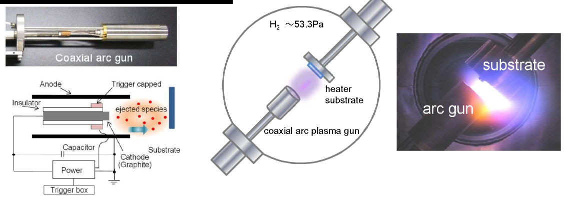

Comparison of deposition methods

Chemical Vapor Deposition

This work
Physical Vapor Deposition

Pulsed Laser Deposition (PLD)
Coaxial Arc Plasma Deposition (CAPD)

	CVD	PVD	
		PLD	CAPD
energy of species	-	from tens to hundreds electron volts	
depo. process	continuous	pulsed	
seeding procedure	required	NOT required	
depo. rate	generally low	80 nm/min	400-6000 nm/min
substrate temp.	700 ~ 1000 °C	550 °C	RT ~ 550 °C
large area depo.	dependent on method	difficult	possible
others	generally high quality	amorphous carbon is cogenerated	

Hydrogen Gas Effect on the UNCD Formation

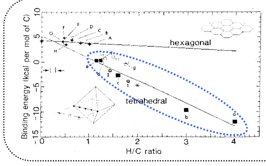

In the case of the dangling bonds of carbon clusters with **diameters less than 3 nm** being terminated by hydrogen, the tetrahedral (diamond) structure is more stable than hexagonal one.

＊ P. Badziag, W. S. Verwoerd, W. P. Ellis and N. R. Greiner, Nature 343 (1990) 244-245.

Hydrogen stabilizes the sp^3 hybridization of carbon atoms at the diamond surface.

＊ M. Frenklach, H. Wang, Phys. Rev. B **43** (1991) 1520.

Atomic hydrogen is involved in the most surface reaction and facilitates the incorporation of carbon atoms into diamond lattices, which results in the enhancement in the deposition rate and crystalline quality.

＊ D. G. Goodin and J. E. Butler, in *Handbook of Industrial Diamonds and Diamond Films*, edited by M. A. Prelas, G. Popovici, and K. Bigelow (Dekker, New York, 1997) p. 527.

Hydrogen atoms remove non-diamond carbon from the surface.

＊ B. V. Spitsyn, L. L. Bouilov, and B. V. Derfaguin, J. Cryst. Growth **52** (1981) 219.

A hydrogen atmosphere might have significant roles on the UNCD formation.

Optical emission measurements of CAPD plasma

CAPD

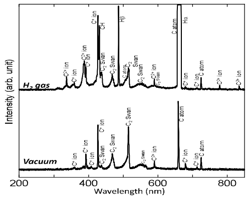

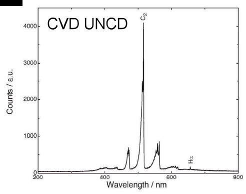

O. A. Williams et al. DRM 15 (2006) 654.

manly from C+ and C species ⟺ dominantly from C_2 swan bands.

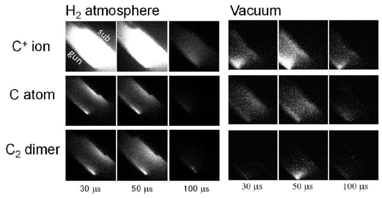

K. Hanada et al. JJAP 49 (2010) 08JF09

Comparison in the process

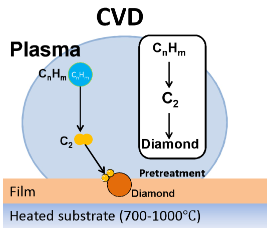

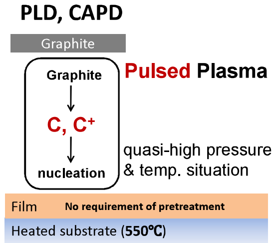

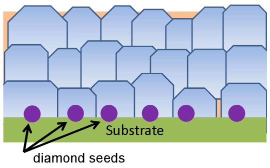

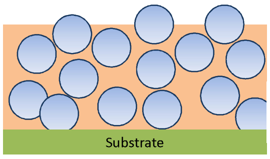

spontaneous growth (nucleation), independently distributed

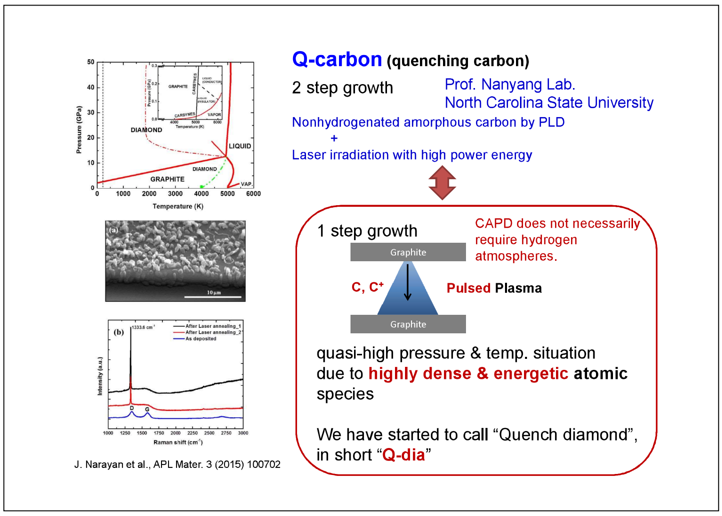

J. Narayan et al., APL Mater. 3 (2015) 100702

Q-carbon **(quenching carbon)**

2 step growth — Prof. Nanyang Lab.
North Carolina State University

Nonhydrogenated amorphous carbon by PLD
+
Laser irradiation with high power energy

1 step growth

CAPD does not necessarily require hydrogen atmospheres.

Pulsed Plasma

quasi-high pressure & temp. situation due to **highly dense & energetic atomic** species

We have started to call "Quench diamond", in short "**Q-dia**"

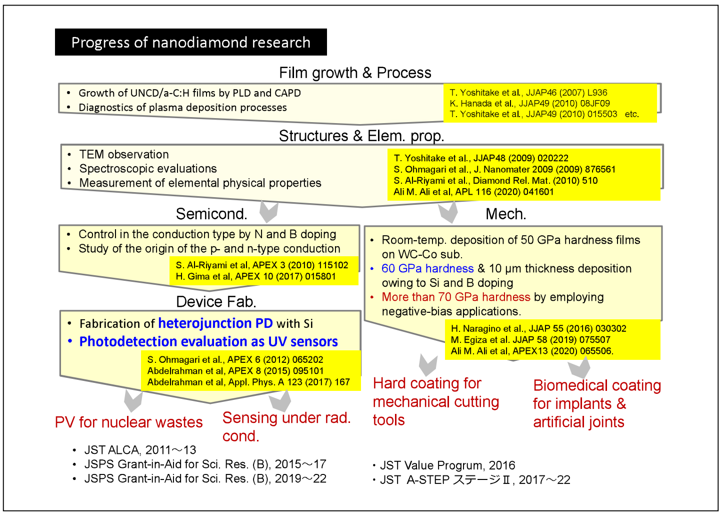

Progress of nanodiamond research

Film growth & Process

- Growth of UNCD/a-C:H films by PLD and CAPD
- Diagnostics of plasma deposition processes

T. Yoshitake et al., JJAP46 (2007) L936
K. Hanada et al., JJAP49 (2010) 08JF09
T. Yoshitake et al., JJAP49 (2010) 015503 etc.

Structures & Elem. prop.

- TEM observation
- Spectroscopic evaluations
- Measurement of elemental physical properties

T. Yoshitake et al., JJAP48 (2009) 020222
S. Ohmagari et al., J. Nanomater 2009 (2009) 876561
S. Al-Riyami et al., Diamond Rel. Mat. (2010) 510
Ali M. Ali et al, APL 116 (2020) 041601

Semicond.

- Control in the conduction type by N and B doping
- Study of the origin of the p- and n-type conduction

S. Al-Riyami et al, APEX 3 (2010) 115102
H. Gima et al, APEX 10 (2017) 015801

Device Fab.

- Fabrication of **heterojunction PD** with Si
- **Photodetection evaluation as UV sensors**

S. Ohmagari et al., APEX 6 (2012) 065202
Abdelrahman et al, APEX 8 (2015) 095101
Abdelrahman et al, Appl. Phys. A 123 (2017) 167

PV for nuclear wastes

Sensing under rad. cond.

- JST ALCA, 2011～13
- JSPS Grant-in-Aid for Sci. Res. (B), 2015～17
- JSPS Grant-in-Aid for Sci. Res. (B), 2019～22

Mech.

- Room-temp. deposition of 50 GPa hardness films on WC-Co sub.
- 60 GPa hardness & 10 µm thickness deposition owing to Si and B doping
- More than 70 GPa hardness by employing negative-bias applications.

H. Naragino et al., JJAP 55 (2016) 030302
M. Egiza et al. JJAP 58 (2019) 075507
Ali M. Ali et al, APEX13 (2020) 065506.

Hard coating for mechanical cutting tools

Biomedical coating for implants & artificial joints

・JST Value Progrum, 2016
・JST A-STEP ステージⅡ, 2017～22

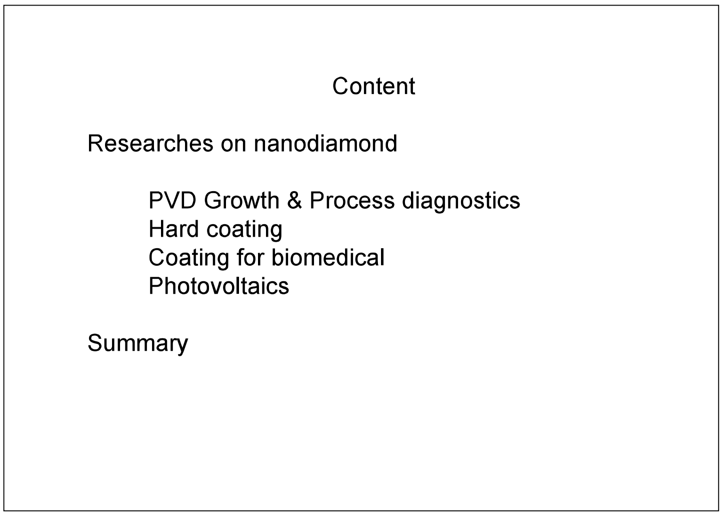

Content

Researches on nanodiamond

PVD Growth & Process diagnostics
Hard coating
Coating for biomedical
Photovoltaics

Summary

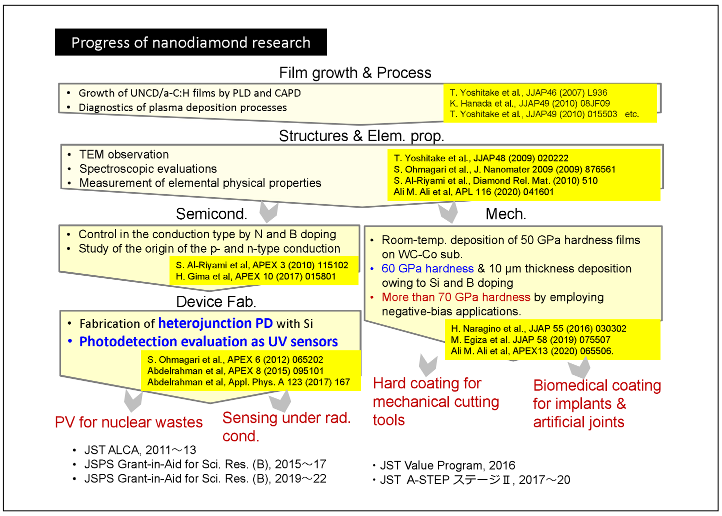

Progress of nanodiamond research

Film growth & Process

- Growth of UNCD/a-C:H films by PLD and CAPD
- Diagnostics of plasma deposition processes

T. Yoshitake et al., JJAP46 (2007) L936
K. Hanada et al., JJAP49 (2010) 08JF09
T. Yoshitake et al., JJAP49 (2010) 015503 etc.

Structures & Elem. prop.

- TEM observation
- Spectroscopic evaluations
- Measurement of elemental physical properties

T. Yoshitake et al., JJAP48 (2009) 020222
S. Ohmagari et al., J. Nanomater 2009 (2009) 876561
S. Al-Riyami et al., Diamond Rel. Mat. (2010) 510
Ali M. Ali et al, APL 116 (2020) 041601

Semicond.

- Control in the conduction type by N and B doping
- Study of the origin of the p- and n-type conduction

S. Al-Riyami et al, APEX 3 (2010) 115102
H. Gima et al, APEX 10 (2017) 015801

Device Fab.

- Fabrication of **heterojunction PD** with Si
- **Photodetection evaluation as UV sensors**

S. Ohmagari et al., APEX 6 (2012) 065202
Abdelrahman et al, APEX 8 (2015) 095101
Abdelrahman et al, Appl. Phys. A 123 (2017) 167

PV for nuclear wastes

Sensing under rad. cond.

- JST ALCA, 2011～13
- JSPS Grant-in-Aid for Sci. Res. (B), 2015～17
- JSPS Grant-in-Aid for Sci. Res. (B), 2019～22

Mech.

- Room-temp. deposition of 50 GPa hardness films on WC-Co sub.
- 60 GPa hardness & 10 µm thickness deposition owing to Si and B doping
- More than 70 GPa hardness by employing negative-bias applications.

H. Naragino et al., JJAP 55 (2016) 030302
M. Egiza et al. JJAP 58 (2019) 075507
Ali M. Ali et al, APEX13 (2020) 065506.

Hard coating for mechanical cutting tools

Biomedical coating for implants & artificial joints

・JST Value Progrum, 2016
・JST A-STEP ステージⅡ, 2017～20

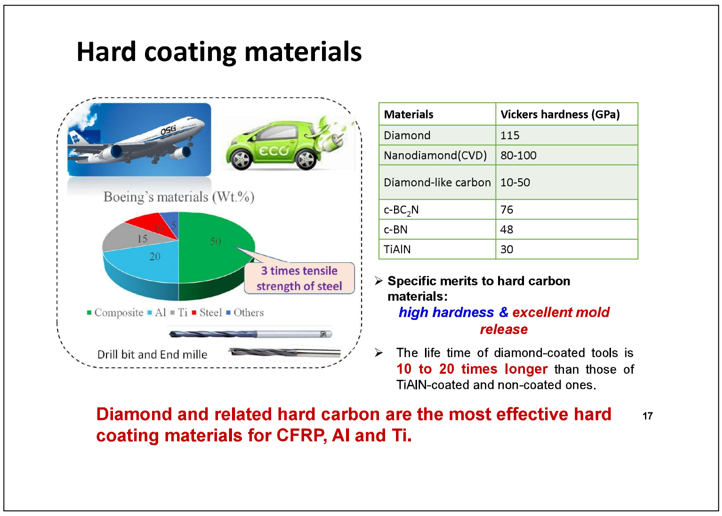

Hard coating materials

Drill bit and End mille

Materials	Vickers hardness (GPa)
Diamond	115
Nanodiamond(CVD)	80-100
Diamond-like carbon	10-50
c-BC_2N	76
c-BN	48
TiAlN	30

- **Specific merits to hard carbon materials:**
  high hardness & excellent mold release
- The life time of diamond-coated tools is **10 to 20 times longer** than those of TiAlN-coated and non-coated ones.

Diamond and related hard carbon are the most effective hard coating materials for CFRP, Al and Ti.

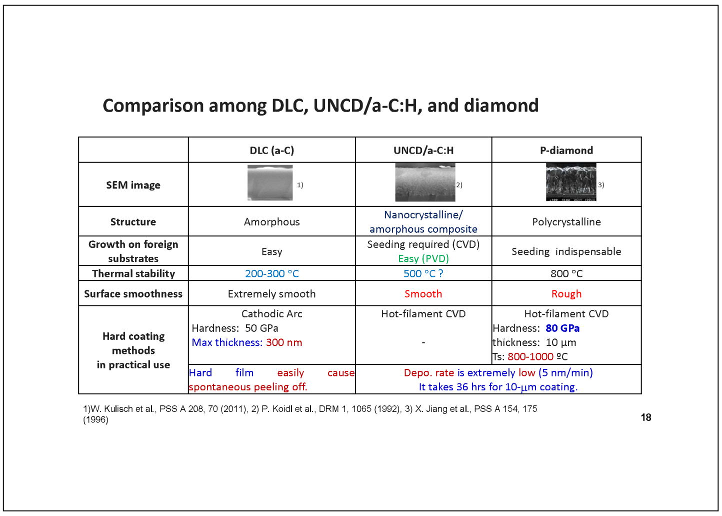

Comparison among DLC, UNCD/a-C:H, and diamond

	DLC (a-C)	UNCD/a-C:H	P-diamond
SEM image	1)	2)	3)
Structure	Amorphous	Nanocrystalline/ amorphous composite	Polycrystalline
Growth on foreign substrates	Easy	Seeding required (CVD) Easy (PVD)	Seeding indispensable
Thermal stability	200-300 °C	500 °C ?	800 °C
Surface smoothness	Extremely smooth	Smooth	Rough
Hard coating methods in practical use	Cathodic Arc Hardness: 50 GPa Max thickness: 300 nm	Hot-filament CVD -	Hot-filament CVD Hardness: **80 GPa** thickness: 10 µm Ts: 800-1000 ºC
	Hard film easily cause spontaneous peeling off.	Depo. rate is extremely low (5 nm/min) It takes 36 hrs for 10-µm coating.	

1)W. Kulisch et al., PSS A 208, 70 (2011), 2) P. Koidl et al., DRM 1, 1065 (1992), 3) X. Jiang et al., PSS A 154, 175 (1996)

Advantages of Coaxial Arc Plasma Deposition (CAPD)

A large number of highly energetic excited carbon species is supplied onto substrate surface.

Schematic of deposition process of CAPD

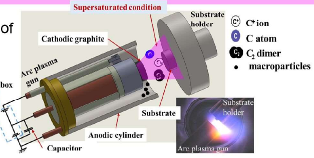

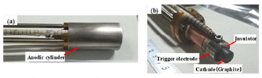

Coaxial arc plasma gun of CAPD (a) with and (b) without the anodic cylinder

Typical image of CAPD machine

Advantages of Coaxial Arc Plasma Deposition (CAPD)

UNCD/a-C coating by CAPD	DLC coating by cathodic arc deposition	polycrystalline diamond coating by HF-CVD
Depo. rate is extremely large: > 500 nm/min The deposition time can drastically be shortened.	comparable or slightly larger	5 nm/min
R.Ts growth is possible. Co catalytic effects can be minimized.		Ts: 800-1000 ºC Co removal on WC-Co surface by acid is indispensable prior to coating. Serious problem in prac. use
UNCD/a-C coating by CAPD on WC-Co has **never** been tried thus far. **What are its merits as hard coating materials?**	Representative method Technically established	

Research target

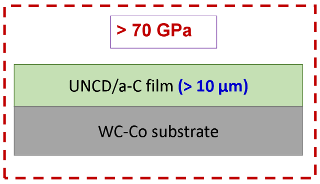

> 70 GPa

UNCD/a-C film **(> 10 µm)**

WC-Co substrate

2017-2020
JST A-STEP Stage II (seed development type AS2915051S)

Experimental Procedures

- ○ The surface of WC-Co substrates was mainly roughened prior to deposition.
- ○ The etching of Co on the surface was NOT carried out.
- ○ Undoped UNCD/a-C films were deposited on WC-Co at RT and 1 Hz repetition rate.
- ○ Si & B-doped UNCD/a-C films were deposited directly on the WC-Co substrate at various concentration of Si & B, and after inserting 1μm UNCD/a-C buffer layer.

Characterizations of films

- ○ XRD, SEM, PES (Saga-LS), EDX, SIMS, wear test, internal stress and nanoindentation

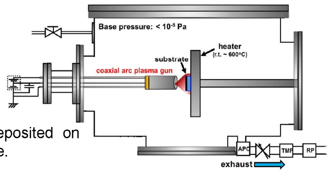

Schematic diagram of CAPD

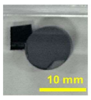

Typical image of the deposit

Undoped UNCD/a-C films: Hardness & Diamond formation

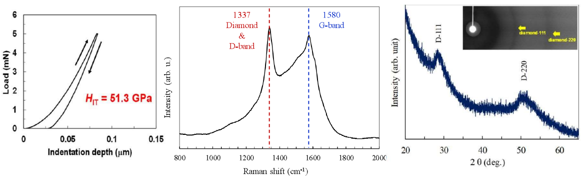

- The film deposited at RT achieved hardness of **51 GPa**, which corresponds to the max hardness of hydrogen-free DLC.
- Raman spectra indicates the formation of diamond.
- The crystallite size was estimated from XRD measurements to be **2.4** nm .

Co diffusion into films

SIMS depth-profile of Co indicates that **Co atoms hardly diffuse into films even at Ts = 550 °C.**

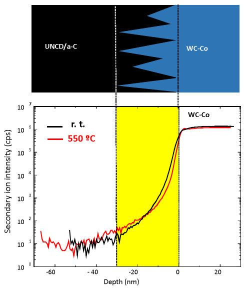

Comparison in SIMS depth-profile of Co between the films deposited at room temp. and 550 ºC. (Yellow-colored range refers to surface roughness regions of WC-Co substrates)

Diamond growth & Co diffusion into the films

The EDX depth profiles also confirm that the Co atoms in WC-Co hardly diffuse into the film even at Ts = 550 °C.

1. The substrate temperature (RT-550°C) is much lower than that (800-1000°C) of HF-CVD.
2. Since the CAPD deposition is depending on pulsed process, an increase in Ts might be suppressed.

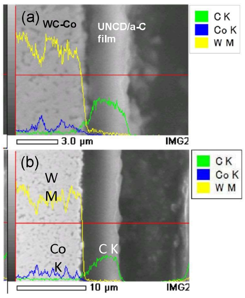

Cross-sectional SEM image and EDX signal depth profiles of C,W, and Co of films deposited at (a) R.T. and (b) 550 °C

Undoped UNCD/a-C films: Internal stress & film thickness

- The UNCD/a-C coating achieved **more than 10 μm** film thickness which is two order larger comparably to the hard DLC (**300 nm**)
- The internal stress was estimated to be only 4.5 GPa, which is much smaller than that of comparably hard DLC.
- The low value of the internal stress can be attributed to the large amount of GBs.

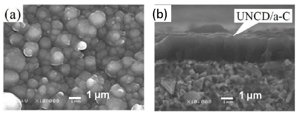

SEM images of UNCD/a-C film (a) Top and (b) cross-sectional view

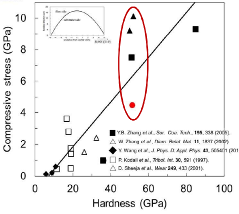

Comparison of stress between DLC and UNCD/a-C films

Si or B doping effects

- ☐ Si doping facilitate the diffusion of Co atoms from the WC-Co substrates into the films.
  - → Owing to the catalytic effects of Co atoms, the sp2 content increases and the hardness was degraded.
- ☐ Undoped UNCD/a-C buffer layers is effective for the suppression of the Co diffusion.
- ☐ Si doping has effects of enhancing the hardness (60 GPa) and Young's modules (600 GPa).
  - By employing undoped UNCD/a-C buffer layers, the Si-doped films exhibited the hardness of 60 GPa.
- ☐ B doping has effects similarly to Si doping

Mohamed Egiza et al., JJAP 58 (2019) 075507.

Negative bias effects

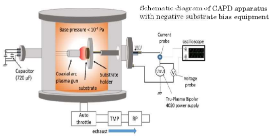

Schematic diagram of CAPD apparatus with negative substrate bias equipment

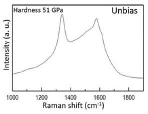

Negative bias

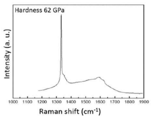

Depo. rate:
2-3 times larger

77 GPa hardness achieved!

Patent, under preparation

Content

Researches on nanodiamond

PVD Growth & Process diagnostics
Hard coating
Coating for biomedical
Photovoltaics

Summary

Applications of diamond coating to implants and artificial joints

Background Size of markets of implants and artificial joints is 3.4 billions yen in 2011 and expected to be 4-5 billions yen at present.

<Implants> Ti is basic material. Corrosion resistance of Ti against saliva is problem to be solved.

Ti corrosion shortens implant life time.

Metals except for Ti possess low affinities for living bodies.

→Corrosion suppressison by coating is required.

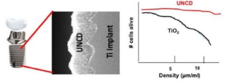

Nanodiamond coating improves corrosion for saliva by an order. [B. Patel et al., Surf. Innovations 5 (2017) 106]

<Artificial joints> In addition to present joints, new-type joints comprising pairs of ceramics and metals are under development.

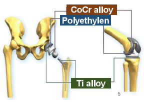

High affinities for living bodies: required for basic materials and abrasion powder
Even if CoCr alloys are passivated, their abrasion powder is toxic.
Metallic ions have risk of cell toxicity.

Low sliding friction: Hard, low friction, and smooth surface are preferable.
Metals and ceramics have sliding frictions.

High abrasion and corrosion resistances: mechanically and chemically tough
It is difficult for metals and ceramics to satisfy both resistances.

→ Hard carbon coating is a promising candidate for solving above-mentioned problems.

Applications of diamond coating to implants and artificial joints

	DLC	NCD	Diamond(PCD)
SEM images	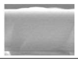 1)	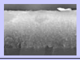 2)	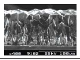 3)
Structure	Amorphous	Nanocrystals/amorphous	polycrystalline
Deposition method	Ion plating deposition (PVD)	MWCVD CAPD (PVD)	HFCVD (CVD)
Sub. Temp.	200～300 ˚C	**Room temp.**	800～900 ˚C
Surf. roughness	Smooth	Smooth	Rough
Hardness	50～60 GPa	> 50 GPa	90～120 GPa
Thickness	< 0.5 μm	**> 10 μm**	> 10 μm
Depo. rate	0.5～2μm/h	**> 3 μm/h**	0.5 μm /h

1)W. Kulisch et al., PSSA 208,70 (2011), 2) P. Koidl et al., DRM 1, 1065 (1992), 3) X. Jianget al., PSSA 154, 175 (1996)

Diamond possesses the lowest thermal exp coefficient 8×10^{-7} K^{-1} among materials, which is more than an order of magnitude larger than those of metallic basic materials such as Ti.

Owing to the room-temperature growth, the deposition of films w/o peeling off is realized.

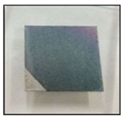

Collab w/ KU Hospital Implant Center

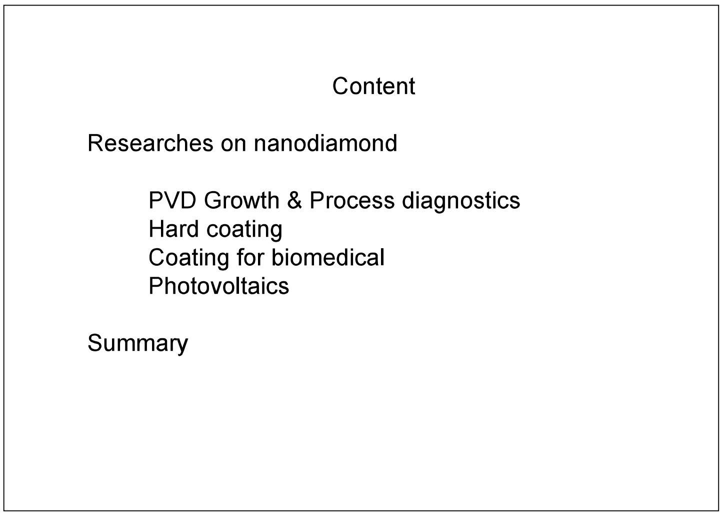

Content

Researches on nanodiamond

PVD Growth & Process diagnostics
Hard coating
Coating for biomedical
Photovoltaics

Summary

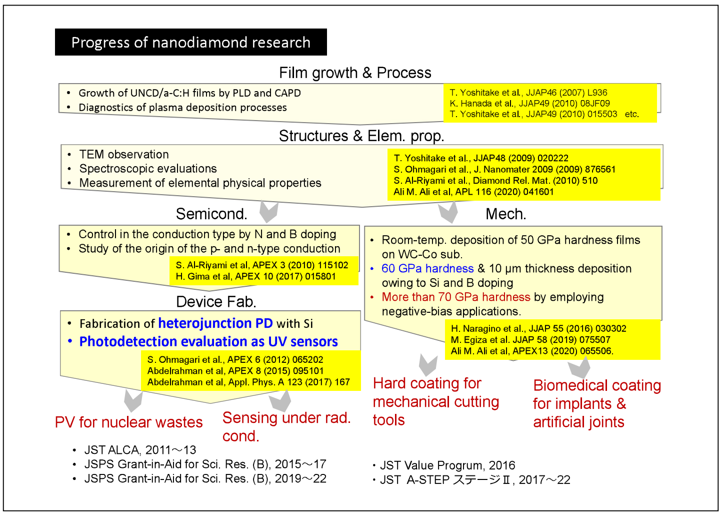

Progress of nanodiamond research

Film growth & Process

- Growth of UNCD/a-C:H films by PLD and CAPD
- Diagnostics of plasma deposition processes

T. Yoshitake et al., JJAP46 (2007) L936
K. Hanada et al., JJAP49 (2010) 08JF09
T. Yoshitake et al., JJAP49 (2010) 015503 etc.

Structures & Elem. prop.

- TEM observation
- Spectroscopic evaluations
- Measurement of elemental physical properties

T. Yoshitake et al., JJAP48 (2009) 020222
S. Ohmagari et al., J. Nanomater 2009 (2009) 876561
S. Al-Riyami et al., Diamond Rel. Mat. (2010) 510
Ali M. Ali et al, APL 116 (2020) 041601

Semicond.

- Control in the conduction type by N and B doping
- Study of the origin of the p- and n-type conduction

S. Al-Riyami et al, APEX 3 (2010) 115102
H. Gima et al, APEX 10 (2017) 015801

Device Fab.

- Fabrication of **heterojunction PD** with Si
- **Photodetection evaluation as UV sensors**

S. Ohmagari et al., APEX 6 (2012) 065202
Abdelrahman et al, APEX 8 (2015) 095101
Abdelrahman et al, Appl. Phys. A 123 (2017) 167

PV for nuclear wastes

Sensing under rad. cond.

- JST ALCA, 2011～13
- JSPS Grant-in-Aid for Sci. Res. (B), 2015～17
- JSPS Grant-in-Aid for Sci. Res. (B), 2019～22

Mech.

- Room-temp. deposition of 50 GPa hardness films on WC-Co sub.
- 60 GPa hardness & 10 μm thickness deposition owing to Si and B doping
- More than 70 GPa hardness by employing negative-bias applications.

H. Naragino et al., JJAP 55 (2016) 030302
M. Egiza et al. JJAP 58 (2019) 075507
Ali M. Ali et al, APEX13 (2020) 065506.

Hard coating for mechanical cutting tools

Biomedical coating for implants & artificial joints

- JST Value Progrum, 2016
- JST A-STEP ステージⅡ, 2017～22

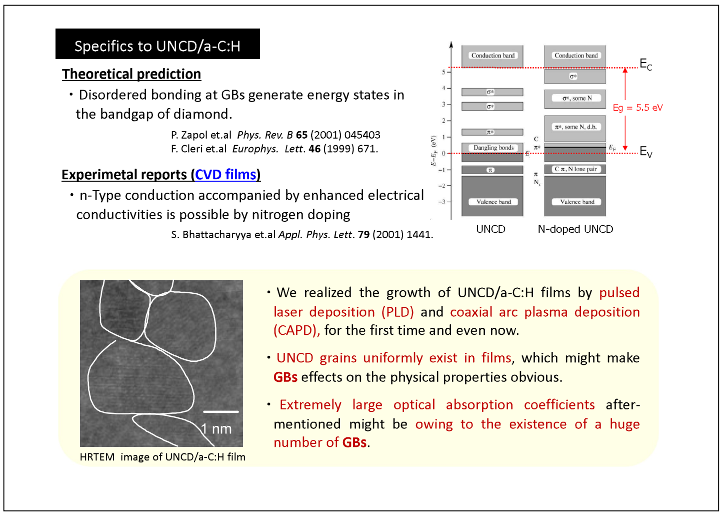

Specifics to UNCD/a-C:H

Theoretical prediction

- Disordered bonding at GBs generate energy states in the bandgap of diamond.

P. Zapol et.al *Phys. Rev. B* **65** (2001) 045403
F. Cleri et.al *Europhys. Lett.* **46** (1999) 671.

Experimetal reports (CVD films)

- n-Type conduction accompanied by enhanced electrical conductivities is possible by nitrogen doping

S. Bhattacharyya et.al *Appl. Phys. Lett.* **79** (2001) 1441.

HRTEM image of UNCD/a-C:H film

- We realized the growth of UNCD/a-C:H films by pulsed laser deposition (PLD) and coaxial arc plasma deposition (CAPD), for the first time and even now.
- UNCD grains uniformly exist in films, which might make **GBs** effects on the physical properties obvious.
- Extremely large optical absorption coefficients after-mentioned might be owing to the existence of a huge number of **GBs**.

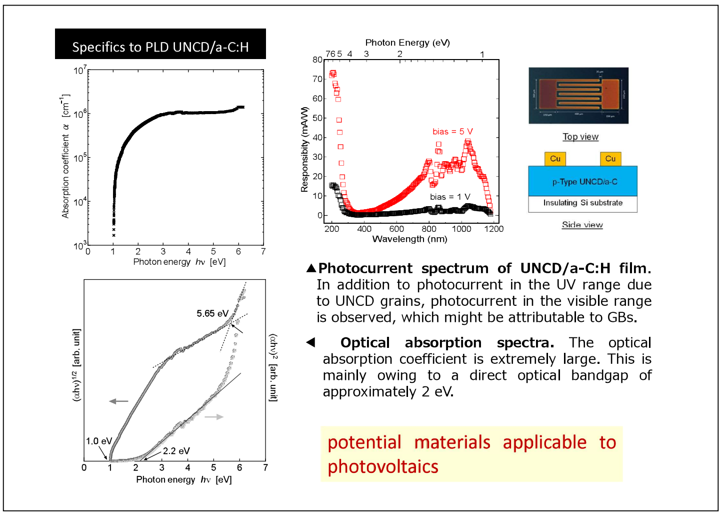

Specifics to PLD UNCD/a-C:H

▲**Photocurrent spectrum of UNCD/a-C:H film.** In addition to photocurrent in the UV range due to UNCD grains, photocurrent in the visible range is observed, which might be attributable to GBs.

◀ **Optical absorption spectra.** The optical absorption coefficient is extremely large. This is mainly owing to a direct optical bandgap of approximately 2 eV.

potential materials applicable to photovoltaics

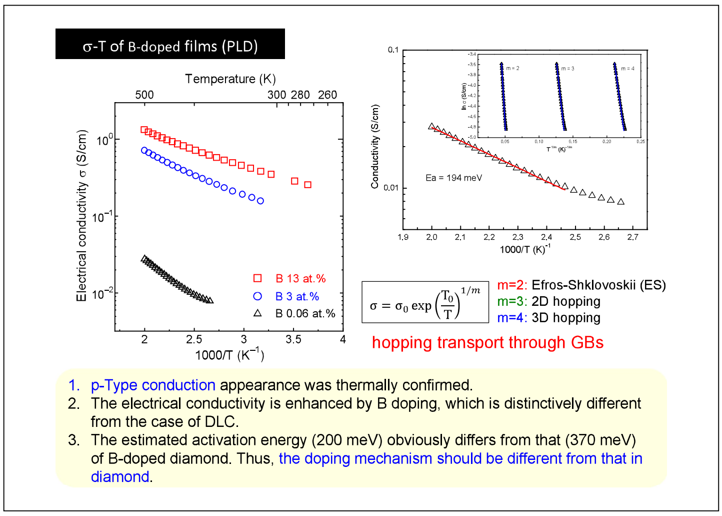

σ-T of B-doped films (PLD)

$$\sigma = \sigma_0 \exp\left(\frac{T_0}{T}\right)^{1/m}$$

m=2: Efros-Shklovoskii (ES)
m=3: 2D hopping
m=4: 3D hopping

hopping transport through GBs

1. p-Type conduction appearance was thermally confirmed.
2. The electrical conductivity is enhanced by B doping, which is distinctively different from the case of DLC.
3. The estimated activation energy (200 meV) obviously differs from that (370 meV) of B-doped diamond. Thus, the doping mechanism should be different from that in diamond.

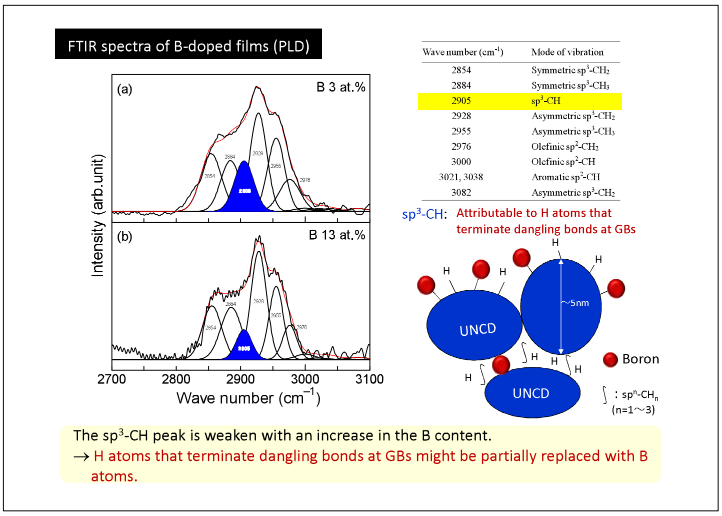

FTIR spectra of B-doped films (PLD)

Wave number (cm^{-1})	Mode of vibration
2854	Symmetric sp^3-CH_2
2884	Symmetric sp^3-CH_3
2905	sp^3-CH
2928	Asymmetric sp^3-CH_2
2955	Asymmetric sp^3-CH_3
2976	Olefinic sp^2-CH_2
3000	Olefinic sp^2-CH
3021, 3038	Aromatic sp^2-CH
3082	Asymmetric sp^3-CH_2

sp^3-CH: Attributable to H atoms that terminate dangling bonds at GBs

The sp^3-CH peak is weaken with an increase in the B content.
→ H atoms that terminate dangling bonds at GBs might be partially replaced with B atoms.

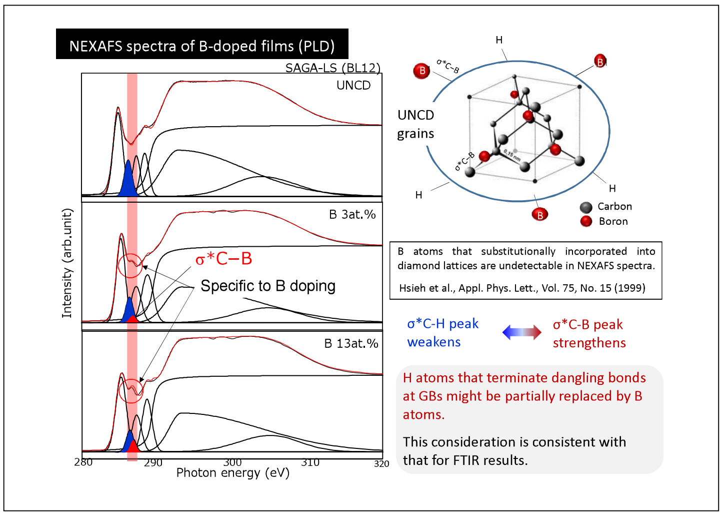

NEXAFS spectra of B-doped films (PLD)

B atoms that substitutionally incorporated into diamond lattices are undetectable in NEXAFS spectra.

Hsieh et al., Appl. Phys. Lett., Vol. 75, No. 15 (1999)

σ*C-H peak weakens ⇔ σ*C-B peak strengthens

H atoms that terminate dangling bonds at GBs might be partially replaced by B atoms.

This consideration is consistent with that for FTIR results.

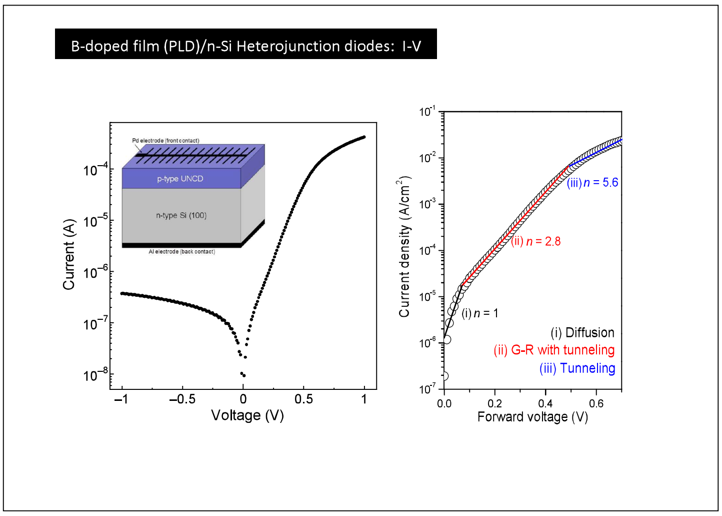

B-doped film (PLD)/n-Si Heterojunction diodes: I-V

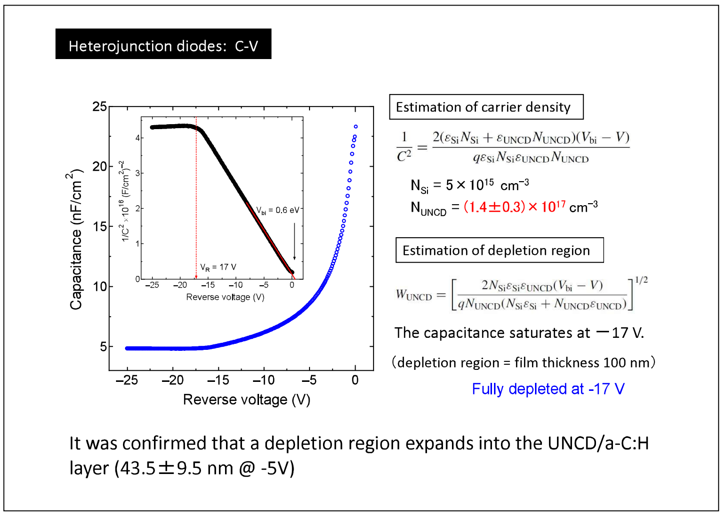

Heterojunction diodes: C-V

Estimation of carrier density

$$\frac{1}{C^2} = \frac{2(\varepsilon_{\mathrm{Si}} N_{\mathrm{Si}} + \varepsilon_{\mathrm{UNCD}} N_{\mathrm{UNCD}})(V_{\mathrm{bi}} - V)}{q \varepsilon_{\mathrm{Si}} N_{\mathrm{Si}} \varepsilon_{\mathrm{UNCD}} N_{\mathrm{UNCD}}}$$

$N_{Si} = 5 \times 10^{15}$ cm^{-3}

$N_{UNCD} = (1.4 \pm 0.3) \times 10^{17}$ cm^{-3}

Estimation of depletion region

$$W_{\mathrm{UNCD}} = \left[\frac{2 N_{\mathrm{Si}} \varepsilon_{\mathrm{Si}} \varepsilon_{\mathrm{UNCD}} (V_{\mathrm{bi}} - V)}{q N_{\mathrm{UNCD}} (N_{\mathrm{Si}} \varepsilon_{\mathrm{Si}} + N_{\mathrm{UNCD}} \varepsilon_{\mathrm{UNCD}})}\right]^{1/2}$$

The capacitance saturates at −17 V.

(depletion region = film thickness 100 nm)

Fully depleted at -17 V

It was confirmed that a depletion region expands into the UNCD/a-C:H layer (43.5±9.5 nm @ -5V)

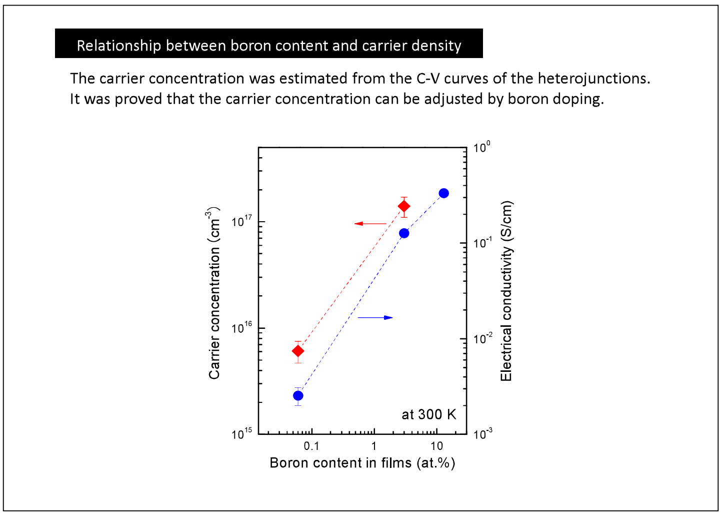

Relationship between boron content and carrier density

The carrier concentration was estimated from the C-V curves of the heterojunctions.
It was proved that the carrier concentration can be adjusted by boron doping.

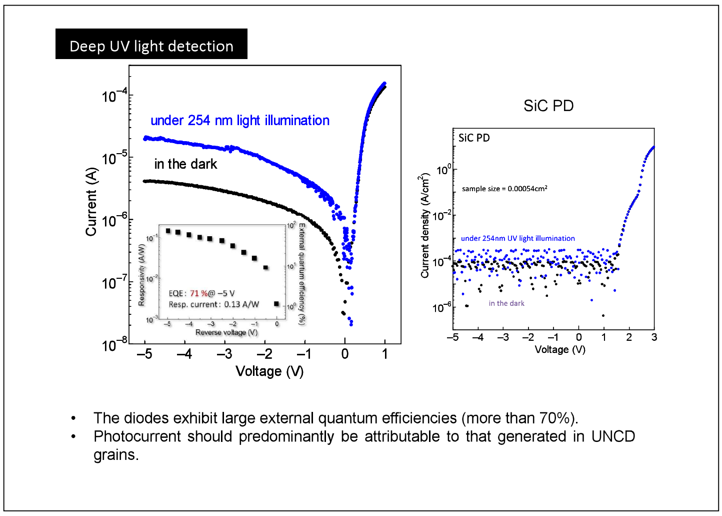

Deep UV light detection

- The diodes exhibit large external quantum efficiencies (more than 70%).
- Photocurrent should predominantly be attributable to that generated in UNCD grains.

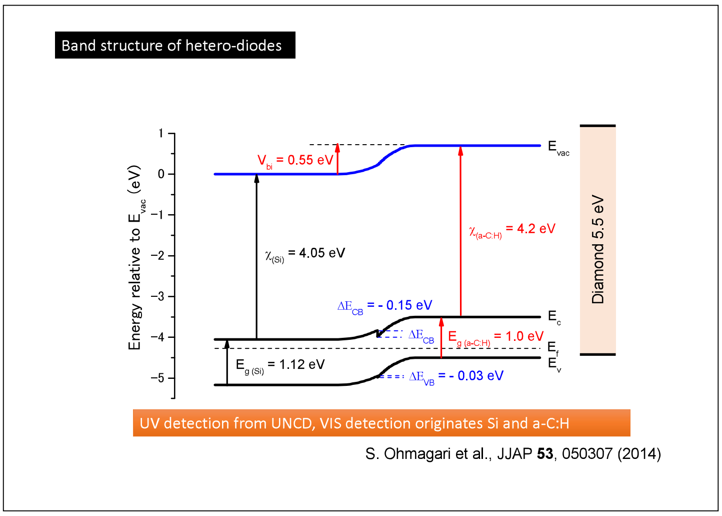

Band structure of hetero-diodes

UV detection from UNCD, VIS detection originates Si and a-C:H

S. Ohmagari et al., JJAP **53**, 050307 (2014)

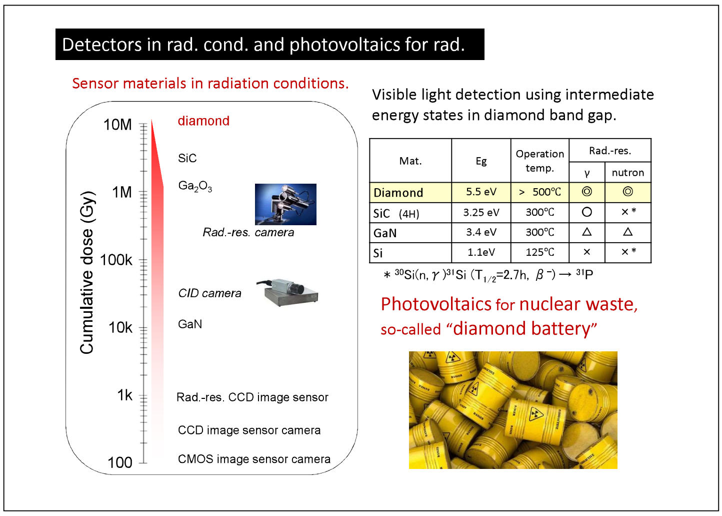

Detectors in rad. cond. and photovoltaics for rad.

Sensor materials in radiation conditions.

Visible light detection using intermediate energy states in diamond band gap.

Mat.	Eg	Operation temp.	Rad.-res.	
			γ	nutron
Diamond	5.5 eV	> 500℃	◎	◎
SiC (4H)	3.25 eV	300℃	○	×*
GaN	3.4 eV	300℃	△	△
Si	1.1eV	125℃	×	×*

* $^{30}Si(n,\gamma)^{31}Si\ (T_{1/2}=2.7h,\ \beta^-) \rightarrow {}^{31}P$

Photovoltaics for nuclear waste, so-called "diamond battery"

Summary

Our nanodiamond research (Q-dia), which we have constructively progressed step by step thus far, was introduced. We are prospecting followings for each application.

- ❑ PVD Growth & Process diagnostics
  Owing to process developments, the film quality is comparable with that of CVD nanodiamond, in spite of room temperature deposition.
- ❑ Photovoltaics
  Heterojunctions with SC diamond will be prepared, and we consider their application to detectors under radiation conditions and PV for nuclear wastes.
- ❑ Hard coating
  More than 70 GPa hardness and more than 10 μm-thickness deposition are achieved for WC-Co. Practical use is under consideration with a mechanical tool company.
- ❑ Coating for biomedical
  Deposition on Ti is achieved. The biomedical effectiveness will be studied with KU Hospital Implant Center.

Thank you for your kind attention !

- ❑ This research was partially financially supported by JST A-STEP Stage II (seed development type AS2915051S) and JSPS KAKENHI (Grant number JP19H02436).
- ❑ The X-ray measurements were performed at Kyushu Synchrotron Light Research Center/Saga Light Source (Proposal Nos. 1804026S, 1901139S, 1905035S, 1908066S, and 1911112S).